AIChE

Assessment of Physiological Conditions in *E. Coli* Fermentations by Epifluorescent Microscopy and Image Analysis

Sónia Carneiro
Centre of Biological Engineering, IBB-Institute for Biotechnology and Bioengineering, Universidade do Minho, Campus de Gualtar, 4710-057 Braga, Portugal

António L. Amaral
Centre of Biological Engineering, IBB-Institute for Biotechnology and Bioengineering, Universidade do Minho, Campus de Gualtar, 4710-057 Braga, Portugal

Departamento de Engenharia Química e Biológica, Instituto Superior de Engenharia de Coimbra, Instituto Politécnico de Coimbra, Rua Pedro Nunes, Quinta da Nora, 3030-199 Coimbra, Portugal

Ana C. A. Veloso
Centre of Biological Engineering, IBB-Institute for Biotechnology and Bioengineering, Universidade do Minho, Campus de Gualtar, 4710-057 Braga, Portugal

CIMO - Escola Superior Agrária de Bragança, Instituto Politécnico de Bragança, Campus de Santa Apolónia, Apartado 1172, 5301-855 Bragança, Portugal

Departamento de Engenharia Química e Biológica, Instituto Superior de Engenharia de Coimbra, Instituto Politécnico de Coimbra, Rua Pedro Nunes, Quinta da Nora, 3030-199 Coimbra, Portugal

Teresa Dias
CIMO - Escola Superior Agrária de Bragança, Instituto Politécnico de Bragança, Campus de Santa Apolónia, Apartado 1172, 5301-855 Bragança, Portugal

António M. Peres
CIMO - Escola Superior Agrária de Bragança, Instituto Politécnico de Bragança, Campus de Santa Apolónia, Apartado 1172, 5301-855 Bragança, Portugal

LSRE-Escola Superior Agrária de Bragança, Instituto Politécnico de Bragança, Campus de Santa Apolónia, Apartado 1172, 5301-855 Bragança, Portugal

Eugénio C. Ferreira and Isabel Rocha
Centre of Biological Engineering, IBB-Institute for Biotechnology and Bioengineering, Universidade do Minho, Campus de Gualtar, 4710-057 Braga, Portugal

DOI 10.1002/bp.134
Published online June 3, 2009 in Wiley InterScience (www.interscience.wiley.com).

The development of monitoring methods for assessing the physiological state of microorganisms during recombinant fermentation processes has been encouraged by the need to evaluate the influence of processing conditions in recombinant protein production. In this work, a technique based on microscopy and image analysis was developed that allows the simultaneous quantification of parameters associated with viability and fluorescent protein production in recombinant Escherichia coli fermentations. Images obtained from light microscopy with phase contrast are used to assess the total number of cells in a given sample and, from epifluorescence microscopy, both protein producing and injured cells are evaluated using two different fluorochromes: propidium iodide and enhanced yellow fluorescent protein. This technique revealed the existence of different cell populations in the recombinant E. coli fermentation broth that were evaluated along four batch fermentations, complementing information obtained with standard techniques to study the effects of the temperature and induction time in recombinant protein production processes. © 2009 American Institute of Chemical Engineers *Biotechnol. Prog.*, 25: 882–891, 2009
Keywords: Recombinant E. coli fermentations, epifluorescent microscopy, physiology assessment, image analysis

Introduction

The cultivation of microbial strains expressing recombinant proteins has become an increasingly important

Additional Supporting Information may be found in the online version of this article.

Correspondence concerning this article should be addressed to I. Rocha at irocha@deb.uminho.pt.

technique in the field of biotechnology. The gram-negative bacterium *Escherichia coli* has been one of the most commonly used recombinant protein production systems, due to its ability to grow rapidly and up to high densities on inexpensive substrates. Furthermore, it is one of the best characterized systems regarding molecular genetics, physiology and expression systems.[1–3] An *E. coli* expression system contains a set of genetic elements that might affect both the transcriptional and translational aspects of protein production. It must be considered in terms of the codon usage of the target gene, efficient termination of transcription and translation, mRNA stabilization, plasmid copy number, antibiotic selectability, promoter strength and inducibility.[1,4] Many inducible promoters have been developed, which can be triggered by various mechanisms such as temperature shifting, pH changing and addition of chemical inducers. Among these inducible systems, *lac*-based promoters are the most commonly used ones and can be efficiently stimulated by the addition of isopropyl-β-D-thiogalactopyranoside (IPTG). However, the addition of IPTG stimulates several stress responses even in wild-type strains.[5] It was reported[6] that after induction with IPTG, depending on the optical density (OD) of the culture, the number of cells identified as being either stressed or dead increased and the culture growth progression was different when compared with noninduced cells.

Furthermore, the production of recombinant proteins can significantly influence cell metabolism by channeling resources towards the production of the target protein, thereby imposing a metabolic burden and stress to the host cell.[7] In particular, some stress signals associated with cellular regulons, such as a heat-shock-like or unfolded protein response and the stringent response, can be induced during recombinant protein production.[8] Besides, throughout the fermentation processes, recombinant cells can also be submitted to other stress conditions, including nutrient starvation, oxidative stress, and excessive carbon dioxide levels which can decrease growth rates and stimulate acetate formation.[9]

These physiological phenomena can lead to a significant decrease in protein production during fermentation processes, due to a deviation to alternative metabolic pathways of cell maintenance rather than cell reproduction and protein production. It is therefore essential to include the evaluation of the different physiological responses in fermentation monitoring strategies in order to gain a deeper understanding of the production strains characteristics. This information can then be used for mathematical model construction and validation and for designing process control and optimization strategies.

Cellular viability is one of the most relevant physiological parameters to be assessed, because it is directly connected to process productivity. However, traditional methods based on plate counting only allow to assess cell viability by means of culturable cells grown on plates, but depending on the situation, this may represent only a minor fraction of living cells.[10] Over the last decades, many approaches have been employed for distinguish living from nonliving bacterial cells. Currently, with the advent of modern molecular biology techniques, several novel methods have been employed like bioluminescent assays,[11] fluorescent *in situ* hybridization (FISH),[12] optical tweezers,[13] nucleic acid amplification methods (polymerase chain reaction, PCR),[14] reverse transcription-polymerase chain reaction (RT-PCR)[15,16] and nucleic acid sequence-based amplification (NASBA).[17] However, the most widely used approaches are fluorescence-based methods either using microscopy[18–20] or flow cytometry.[6,21–24]

In Epifluorescent microscopy (EFM) methods, indicators of viability may be based on different approaches,[25] such as enzymatic activity, membrane integrity, and membrane electrochemical potential. Membrane integrity is one of the most common and is based on the capacity of cells with intact membranes to exclude fluorescent dye compounds, when used at low concentrations. Because of the fact that nucleic acid stains exhibit a large enhancement of fluorescence upon binding, and since those molecules are present in the cells at high concentrations, nucleic acid stains have been widely used for membrane integrity assays.[21,26,27] A wide diversity of membrane impermeant nucleic acid stains can be used, like Sytox® Green or propidium iodide (PI). PI binds to DNA by intercalating between the bases with little or no sequence preference and with a stoichiometry of one dye per 4–5 DNA base pairs. Since it freely penetrates damaged membranes, it is usually considered to be a good cell death indicator, and nonstained cells also include those considered to be in a viable but nonculturable state.[10,28]

During recombinant protein production, besides viability assessment, it is important to measure not only the total amount of product obtained, but also to evaluate the fraction of producing and nonproducing cells, mainly in order to evaluate parameters related to strain performance, like promoter strength and plasmid stability. For this purpose, fluorescent microscopy can also be used if the target protein exhibits fluorescent properties, like the model protein GFP (Green Fluorescent Protein) of the jellyfish *Aequorea victoria* and its derivatives. GFP needs no substrates or cofactors to fluoresce,[29,30] enabling detection by nondestructive means. It is an excellent choice for diverse cell research, having its applications increased widely in recent years.[31,32] Fluorescent proteins are commonly used as reporters for a protein of interest, normally by tagging the fluorescent protein reporter to the protein of interest via genetic fusion.[33–35] An advantage of using GFP as a cellular marker is its stability. In fact, GFP fluorescence can persist even after cell death.[36] In addition, the fact that GFP fluorescence can be easily detectable makes it a very attractive tool for optimizing purification techniques of recombinant proteins and for monitoring protein folding.

However, although fluorescence-based microscopic methods have remained very useful for a wide diversity of applications ranging from industrial to environmental microbiology, for many years the counting of cells from microscopic images has been done manually. Image analysis has therefore become a valuable accessory for such quantifications because it reduces subjectivity and allows automation.[19,37–39] In some fields, such as in fermentation technology, image analysis is now essential for characterizing the physiological state of the culture and for decreasing analytical costs, making microscopy a more practical technique.

The purpose of this study was to establish a rapid, simple, and accurate direct method to evaluate bacterial viability parameters, and protein production during fermentation processes. A dual marker system based on the expression of a GFP variant and PI staining has been used for that purpose.

Materials and Methods

Cultivation conditions

A modified *E. coli* M15 (Qiagen—Germany) with the insertion of the EYFP (Enhanced Yellow Fluorescent

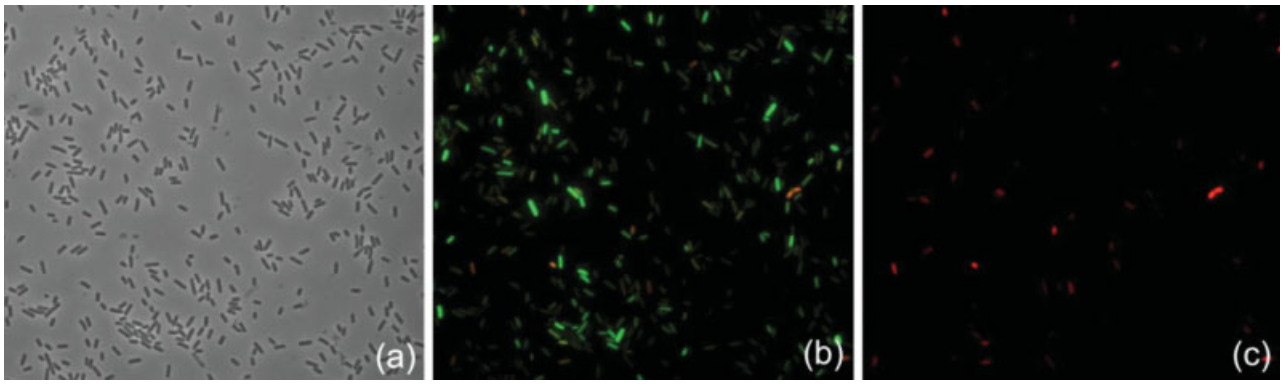

Figure 1. The same sample observed using the various methods.

Contrast-phase microscopy representing all *E. coli* cells (a), epifluorescence microscopy representing EYFP-positive *E. coli* cells (b), and cells stained with propidium iodide (c).

Protein, variant of the *Aequorea victoria* Green Fluorescent Protein) gene in a pEYFP plasmid (Clontech) under the control of a pREP4 plasmid (also from Qiagen) was used. The pUC19 backbone of pEYFP provides a high-copy number origin of replication and an ampicillin resistance gene for propagation and selection in *E. coli*. The multiple copies of pREP4 ensure kanamicin resistance, high levels of *lac* repressor and tight regulation of protein expression. The strain was cultivated in a minimal medium with composition described elsewhere[40] with addition of 0.025 $g \cdot Kg^{-1}$ of kanamycin and 0.1 $g \cdot Kg^{-1}$ ampicillin. Fermentations were conducted in batch mode in a 5 L Biostat MD fermenter from B. Braun Biotech (Germany) equipped with pH, dissolved oxygen (DO) and temperature sensors connected to a digital control unit. The pH of the culture was maintained at 7.0 by automatic addition of 20 M H_3PO_4 or 3.5 M NH_3 by a pH controller. Four batch fermentations were run: fermentations A and B were kept at 33.5°C, while the dissolved oxygen concentration was maintained above 27.5% air saturation; and fermentations C and D were performed at 27 and 40°C, respectively, while the dissolved oxygen concentration was maintained above 40% air saturation. Induction was performed with 1.5 mM of IPTG (isopropyl-β-D-thiogalactopyranoside).

Cell biomass was measured turbidimetrically by optical density at 600 nm in a Jasco V-560 spectrofotometer, calibrated against dry cell weight (DCW, $g \cdot Kg^{-1}$) at 105°C to constant weight. The concentrations of glucose and acetate were measured by HPLC with a refractive index detector (Jasco) and a Chrompack organic acids column (Varian) at 35°C. Analysis of fluorescent protein was performed in a Jasco FP-6200 spectrofluorometer with excitation and emission wavelengths of 513 and 527 nm, respectively, band width of 10 nm each and high sensitivity response in 0.1 sec. Fluorescence intensities are expressed as the mean of two duplicate samples measured in arbitrary fluorescence units (AFUs). These AFUs are considered to be proportional to fluorescent protein accumulated in the cell.

Bacterial staining

Undiluted biomass suspension (100 μL) was mixed with 20 μL of a 0.5 M PI solution and incubated in the dark for 10 min before measurement. A preliminary experiment allowed to conclude that these conditions are sufficient to stain all the injured cells. In fact, all the members of a cell population submitted to high temperatures and high ethanol concentrations were observed to be PI-stained after the image analysis procedure described later. After staining, a drop of the suspension was placed on a glass slide, covered with a cover slip, and sealed with a clear varnish in order to prevent drying of the sample during visualization with the microscope.

Acquisition and analysis of epifluorescence images

The images were acquired in a Zeiss Axioscop microscope (Zeiss, Germany) with a magnification of 1,000 times (1 pixel corresponding to 0.05 μm) coupled with an AxioCam (Zeiss) colour video camera with 1,300 $\times$ 1,030 pixels in 24 bits (8 bits per channel). The colour video camera acquisition parameters (gain, contrast, acquisition time) as well as the microscopy parameters were studied and set at the beginning of the experiment and carefully kept constant. The public domain open source ImageJ 1.33u (NIH) platform was used by the authors to develop the image processing and analysis programmes, that are available for other users upon request.

All population ratios were obtained by means of an image processing and analysis methodology. For that purpose, three sets of images were taken for each sample after staining with PI, choosing representative fields without significant cell aggregation. The first set (bright field *E. coli* images) allows determining the total number of cells in a given image. The second set of images was obtained with a blue filter (wavelength of 450–490 nm) in order to determine the number of EYFP-positive cells (yellow–green cells). Finally the third set of images was obtained with a green filter (wavelength of 534–558 nm) to establish the number of PI-stained cells (red cells). The acquisition methodology consisted on acquiring consecutively the images using the blue filter, the green filter and bright field images.

To determine the total number of cells, the developed software contemplated a preprocessing initial step, followed by background correction, image segmentation, and finally removal of debris smaller than 0.25 μm^2 (see Figure 1).

Regarding the determination of the PI-stained cells (PI^+) the developed programme consisted on background correction of the green filter to eliminate background fluorescence, preprocessing the red channel by masking with the total

E. coli binary image and determination of the PI^+ cells by the enhanced red channel average cell value. The number of cells non stained by PI (PI^-) was then determined by subtracting the PI^+ cells from the total *E. coli* cells (see Supp. Info. for a detailed description of the image analysis methodology).

With respect to the EYFP-positive cells ($EYFP^+$) the programme consisted on background correction of the blue filter image to eliminate background fluorescence, preprocessing the green channel by masking with the total *E. coli* binary image and determination of the $EYFP^+$ cells by the enhanced green channel average cell value.

The determination of the PI stained and EYFP-positive cells (PI^+EYFP^+) consisted in identifying overlapping PI^+ cells in the mask image from red channel and $EYFP^+$ cells in the mask image from green channel and removal of debris smaller than 0.25 μm^2. The number of PI^+EYFP^- and PI^-EYFP^+ cells was determined by subtracting the number of PI^+EYFP^+ cells from the number of PI^+ cells and from the number of $EYFP^+$ cells, respectively. Finally, the number of nonfluorescent cells (PI^-EYFP^-) was determined by subtracting the number of PI^-EYFP^+ cells from the number of PI^- cells.

The programme developed for the determination of the $EYFP^+$ cells also allowed for the calculation of the fluorescence-based image intensity (FII) parameter, directly correlated with the fluorescence of each individual cell. In order to do so, an image of the intensity differences between the red and green channels on the original RGB image had first to be computed. On this image, the FII parameter was obtained by averaging each *E. coli* cell pixel intensity value. The histogram of the *E. coli* cells was further determined for this FII parameter in order to correlate it with the measured AFU for each sample.

Western blot analysis

Equal amounts of protein were separated by SDS-Page using 12.5% polyacrylimide gels according to the method described in.[41] The resolved proteins were electroblotted onto nitocelulose membranes. The membrane was blocked with 5% skim milk in PBS and incubated with an anti-GFP antibody (1 : 500 dilution, BD Living Colors, Clontech Laboratories, Inc.) at room temperature overnight followed by the secondary antibody (1 : 2,000 dilution, BD Living Colors, Clontech Laboratories, Inc.) for 1 hr at room temperature. The protein was detected using α-naftol.

Statistical analysis

All statistical analyzes were carried out in MATLAB 7.1 (Mathworks) and SPSS 17 (Statistical Package for Social Sciences, SPSS Inc.). Normality of the data and homogeneity of variance was studied using Shapiro-Wilk's and Levene's test, respectively. Student's *t*-test was applied in order to study equality of the means. All statistical tests were performed using a 5% significance level.

Results and Discussion

Characterization of the Image Analysis methodology

E. coli samples were taken along several fermentation runs, stained with PI and then visualized by epifluorescent microscopy. Three sets of images (Figure 1) were taken for each sample: bright field *E. coli* images intended to determine the total number of cells; blue filter images in order to determine the number of $EYFP^+$ cells and finally green filter images to establish the number of PI^+ cells. Each set was composed of at least 10 sequential images in order to attain $\sim$ 1,000 of total bacteria. Those images revealed the existence of four different cell populations in the fermentation broth:

1. cells not stained with PI but EYFP positive (referred to as PI^-EYFP^+ cells),
2. nonfluorescent cells (PI^-EYFP^- cells),
3. EYFP and PI positive cells (responding simultaneously to both filters), (PI^+EYFP^+ cells), and
4. cells only responding to the PI filter (PI^+EYFP^- cells).

The corresponding percentages were calculated as the ratio of the number of cells in each population and the total number of cells, as identified by contrast phase microscopy images.

Table 1. Statistical Parameters for Each Cell Population. Mean Standard Deviation and Relative Standard Deviation for PI^+EYFP^-, PI^+EYFP^+, PI^-EYFP^-, and PI^-EYFP^+ Regarding the Results Obtained for Five Replicate Small Samples Taken from the Larger Sample

	Statistical Parameters		
Populations	Mean (%)	Standard Deviation (%)	Variation Coefficient
PI^+EYFP^-	7.1	3.1	0.44
PI^+EYFP^+	20.8	3.9	0.19
PI^-EYFP^-	15.4	2.7	0.18
PI^-EYFP^+	56.7	2.4	0.04

A relevant question to pose when dealing with methodologies that evaluate cellular physiology by looking at individual cells, is if the sample analyzed (usually small, and in this case a drop of cellular suspension) is representative of the entire cellular population inside the bioreactor. A possible approach to evaluate this for the methodology developed here is to investigate the variability of the results obtained within several small samples collected from a larger sample, this one known to represent the entire bioreactor (similar to samples usually taken, for example, to evaluate biomass concentration, which represent around 1% of the reactor volume).

Therefore, a series of five replicate small samples, taken from the same fermentation sample (fermentation D, 21 hr) was carried out, for the evaluation of the four cellular populations described above. The results obtained (mean and standard deviation) for each cell population fraction are presented in Table 1. It was concluded that the four cell fractions present homogeneity of variance ($P > 0.700$, using Levene's test), showing that there is a similar variability associated with production patterns and cellular viability. Nevertheless, it should be noticed that although PI^+EYFP^+, PI^-EYFP^-, and PI^-EYFP^+ cell fractions present acceptable variation coefficient (0.19, 0.18, and 0.04, respectively), PI^+EYFP^- cell fraction shows a higher one (0.44). These results can be partially explained by the natural variability that exists in a cellular population associated with a lower mean, but could be also due to cellular aggregation events that were observed in several samples. In fact, the formed aggregates are sufficient to provoke irregular distribution of cells in the glass slide, which is likely to be the most important variability feature when employing image analysis to enumerate bacterial cells in liquid cultures. Moreover, it was observed, as discussed latter, that cellular aggregation affects more strongly PI^+ cells.

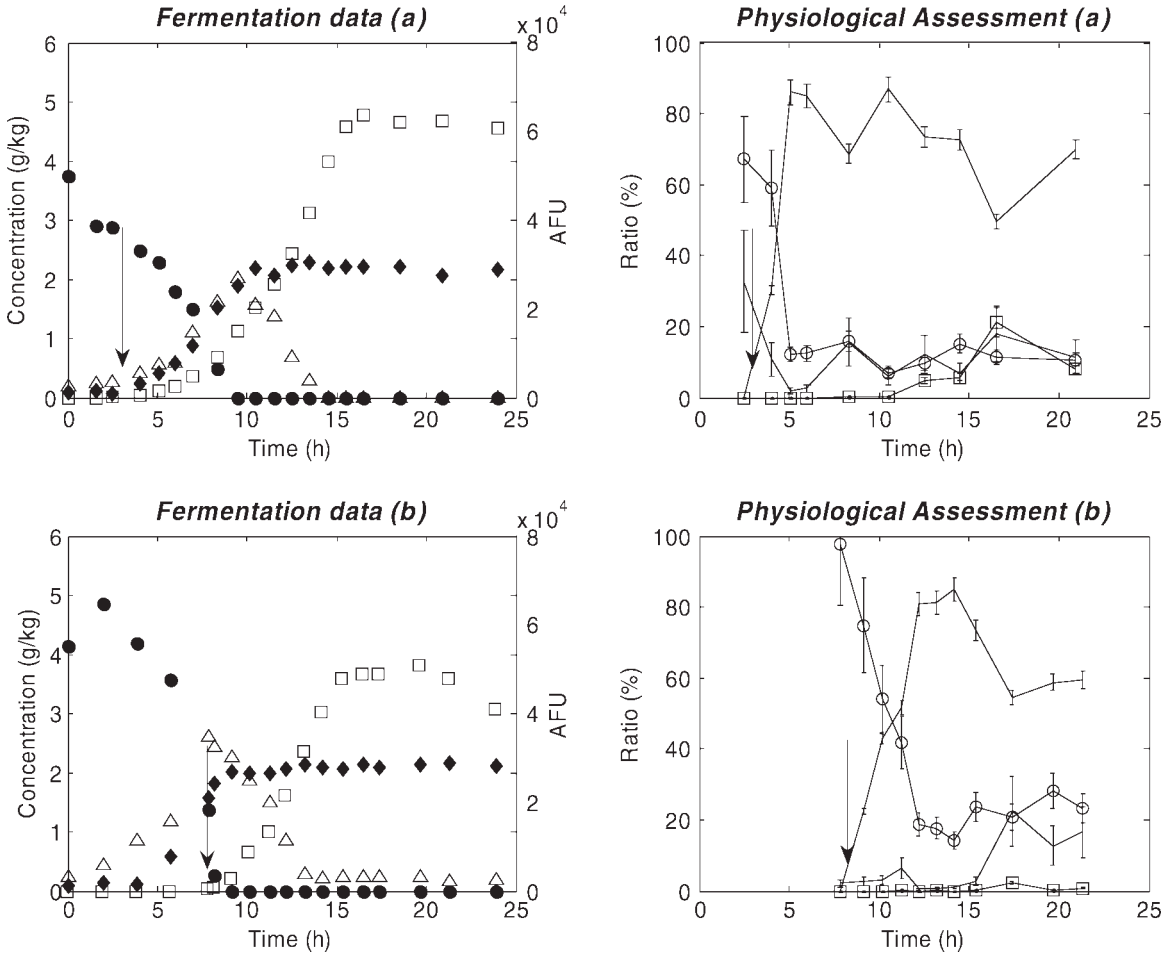

Figure 2. Results obtained in two batch fermentations of *E. coli* induced with IPTG at 2.5 hr (a) and at 8 hr (b) as indicated by the arrow.

Fermentation data illustrates glucose consumption (●), acetate evolution (△), fluorescent protein production (□) and biomass formation (◆), and physiological assessment corresponding to ratios of PI^-EYFP^+ (----), PI^+EYFP^+ (–□–), PI^-EYFP^- (--○--), and PI^+EYFP^- (—) cells, along the fermentation processes.

Given the results obtained regarding the representativeness of the samples, it was relevant to check if the variability obtained within the same sample would allow to distinguish between different samples. For that purpose, a Student's *t*-test for equality of means of two independent samples was performed at significance level of 5%. Data on two samples taken from two different fermentations ran at different temperatures were used. The details on the statistical test performed and on the results obtained are available as Supporting Information.

The analysis revealed a significant difference between both the samples for all populations analyzed ($P < 0.05$). Nevertheless, for PI^+EYFP^+ cell fraction the P value obtained is very close to the usual significance level adopted in statistical studies. Therefore, it can be stated that nevertheless the high standard deviations obtained for some populations (corresponding to high variation coefficient values), it is still possible to use this technique to characterize the physiological states of the cultures.

Fermentation monitoring with EFM and Image Analysis

To illustrate its potential, the described methodology was applied to four batch fermentation runs indicated before. In the first two fermentations (A and B), all conditions were the same, except the time of induction: whereas in fermentation A the induction was performed at the beginning of the exponential phase, in fermentation B cells were already at the end of exponential phase when 1.5 mM of IPTG were added. In the second group of fermentations (fermentations C and D), temperature was the only changed variable, from 27 to 40°C, respectively, being the point of induction the same for both experiments (with regards to biomass concentration). Biomass, carbon source (glucose) and the main by-product (acetate) concentrations are shown in the left-hand panels of Figures 2 and 3, together with arbitrary fluorescent units (AFU) measured with a spectrofluorometer, considered to be proportional to fluorescent protein production. During the course of the fermentations, cell physiology was evaluated by quantifying the different populations defined previously. The first sample taken for cell physiology evaluation was immediately before induction with IPTG. On the right-hand panels of Figures 2 and 3, PI^+EYFP^-, PI^+EYFP^+, PI^-EYFP^-, and PI^-EYFP^+ cell fractions are represented. The main differences between fermentation runs are summarized in Table 2 and dissolved oxygen profiles are available in Supporting Information.

Effect of the moment of induction on physiological parameters

It can be seen from Figure 3 that the time of induction had a clear effect on the progression of the fermentations.

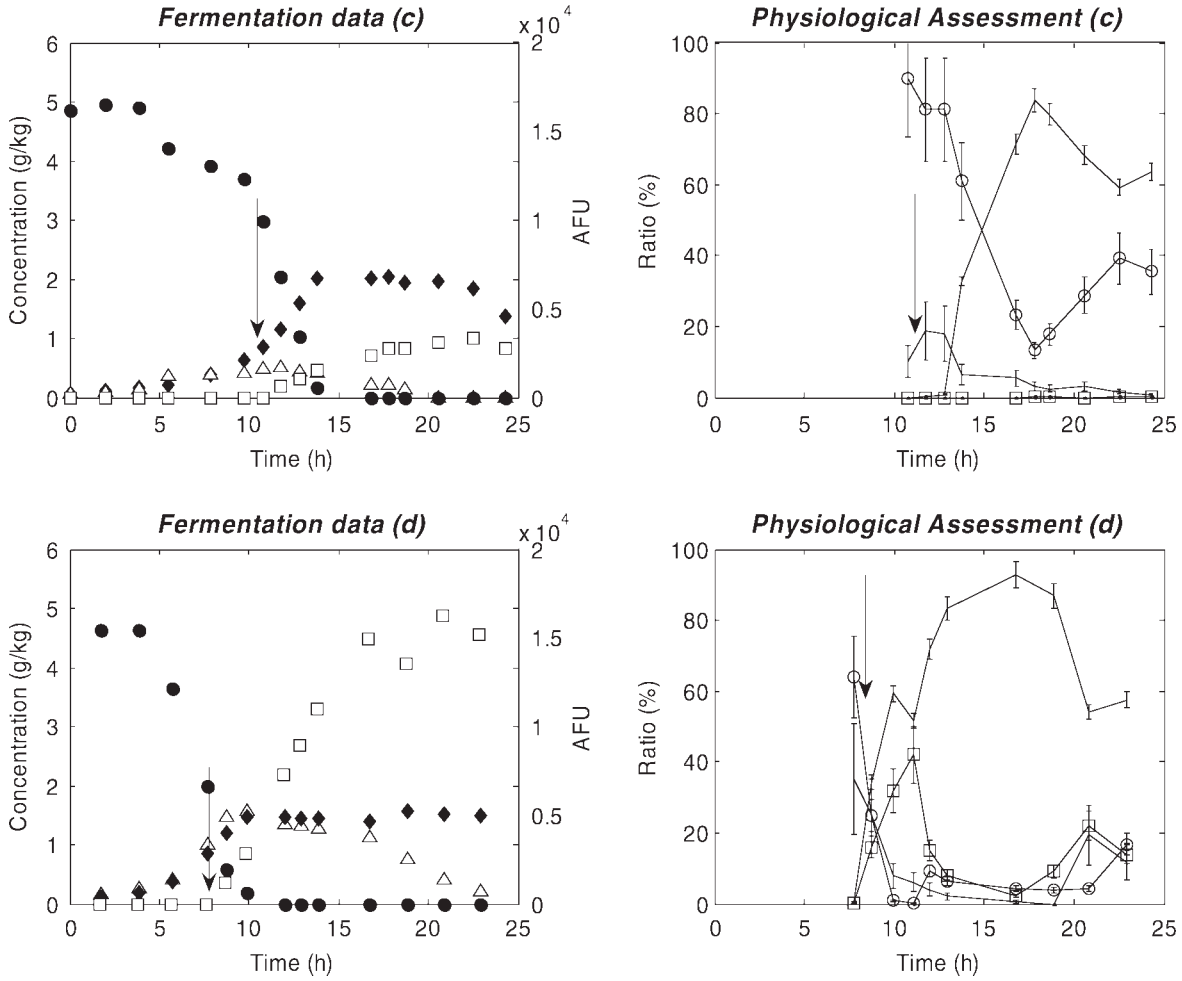

Figure 3. Batch fermentations of *E. coli* performed at 27°C (C) and at 40°C (D), both induced with IPTG at the same O. D., as indicated by the arrow.

Fermentation data illustrate glucose consumption (●), acetate evolution (△), fluorescent protein production (□) and biomass formation (◆), and physiological assessment corresponding to the ratios of PI^-EYFP^+ (----), PI^+EYFP^+ (–□–), PI^-EYFP^- (--○--), and PI^+EYFP^- (—) cells, along the fermentation processes.

Table 2. Experimental Conditions Used in the Fermentations (A–D) with the Corresponding Maxima Achieved Regarding Biomass, Acetate, and Fluorescent Protein

Conditions	A	B	C	D
Temperature (°C)	33.5	33.5	27	40
Dissolved oxygen set point (%)	27.5	27.5	40	40
Induction time (hr)	2.5	8.0	7.8	10.8
Maximum biomass formation (g/kg)	2.28	2.17	2.04	1.57
Maximum acetate production (g/kg)	2.01	2.60	0.50	1.58
Maximum arbitrary fluorescence units	63,710	50,826	33,605	162,660

Regarding recombinant protein production, it is perceptible a higher maximum value for AFU in the earlier induced batch fermentation. It is however clear that AFU values *per se* do not give a broad picture of the production patterns of the culture, as those differences can be due to either an increase in the productivity of individual cells or to an increase in the number of $EYFP^+$ cells, or a combination of both. In this case, image analysis results indicate that the fraction of $EYFP^+$ cells also reaches higher values in the earlier induced fermentation (85% as compared with 80% for PI^-EYFP^+), although this small difference could also be due to the variability observed in the data.

Those facts could be explained by differences in the physiological state of the two cultures at the moment of induction, indicating that in a younger culture the number of cells able to produce recombinant proteins is higher.

It should be emphasized that the presence of a relatively high fraction of PI^-EYFP^- cells after induction is unlikely to be associated with plasmid loss, as the presence of antibiotics throughout the fermentation ensures a strong selective pressure that would rapidly inactivate cells that have lost their plasmids. Therefore, it is plausible that, although possessing plasmids, a significant fraction of the cells in the bioreactor do not produce recombinant proteins probably due to genetic modifications involving the plasmid. In fact, it has been reported that plasmid instability has been related not only to segregational instability induced by defective partitioning of recombinant plasmids during cell division[42] but

also to structural instability caused by point mutations, deletions, insertions and intramolecular rearrangements in the plasmid DNA.[43,44]

Regarding viability, the relative amount of PI^+ cells begins to increase to higher levels for the earlier induced culture. Although it has been reported that the induction effect may be stronger at low OD,[6] leading to cellular stress responses, we have not observed a relationship between the increase in cell death and ITPG addition. There is, however, an obvious increase in the number of PI^+ cells when both glucose and acetate are exhausted, that can be consequence of nutrient starvation. The final ratios of PI^+EYFP^+ and PI^+EYFP^- cells are both close to 20% in fermentation A and, in fermentation B, the PI^+EYFP^- final ratio is around 18% wheras PI^+EYFP^+ ratio is almost zero. Even when nutrients are still present in the fermentation broth, the ratio of PI^+EYFP^- cells in fermentation A is close to 20%. The PI^+EYFP^- cell ratio is likely to be associated with cells that had lost their plasmid and therefore did not produce recombinant protein and, simultaneously, are sensitive to the presence of antibiotic in the fermentation broth. Under this hypothesis, and since this ratio is high during the all fermentation run, it is possible to infer that plasmid loss would occur more strongly for the earlier induced culture, also indicating that protein production and/or IPTG addition may influence plasmid instability, as observed in previous works.[45]

Given the high ratios obtained for PI^+ cells, it is clear that in this process, cell injury cannot be neglected for example for process modeling purposes.

Effect of temperature on physiological parameters

The effect of temperature on recombinant *E. coli* fermentation processes and physiological profiles was investigated, and the results obtained are shown in Figure 3.

The first observation to be drawn from the analysis of Figure 3 is that, although biomass formation is negatively affected by a temperature increase, protein production is significantly enhanced, as the maximum of fluorescence changed from 33,605 AFUs at 27°C to 162,660 AFUs at 40°C. To verify that this fluorescence variation was due to a real increase in fluorescent protein accumulation, and not due to thermosensitivity of the chromophore, a Western blot analysis was performed and results are available as Supporting Information. Additionally, and associated with the increase in recombinant protein production, the total number of $EYFP^+$ cells (as given by the sum of PI^-EYFP^+ and PI^+EYFP^+ cell ratios) was significantly higher for the fermentation performed at 40°C (Student's *t*-test, $P = 0.0015$). In fact, 2 hr after induction, almost 100% of *E. coli* cells were $EYFP^+$ cells, and this ratio was maintained above 90% along 18 hr of fermentation after induction, as compared to values between 80 and 60% for the fermentation carried out at 27°C. For this case, the amount of PI^- cells not expressing the recombinant protein tends to increase along the fermentation, suggesting a less productive expression system and indicating that temperature might affect the control of enzymatic activities related to recombinant protein production.

However, it is clear that the contribution of EYFP producing cells with injured membranes to the global fluorescence intensity at 40°C is very high, as the PI^+EYFP^+ cell ratio increases drastically up to almost 40% of the cellular population 3 hr after induction. This might be closely related with the effect of IPTG induction as has been reported[46] and these cells can be considered as injured cells that still retaining EYFP fluorescence and whose membranes are slightly damaged.[36] However, and probably as cellular lysis takes place, this ratio decreases, indicating that cell injury is mostly related with induction. Nevertheless, there are, during the entire production phase of the fermentation ran at 40°C, higher ratios of PI^+EYFP^+ cells as compared with the experiment conducted at 27°C. Curiously, this trend is not so clear for PI^+EYFP^- cells, since this ratio increased almost 10% after IPTG induction in the fermentation performed at 27°C while a decrease was observed at 40°C.

Moreover, the possible impact of nutrient starvation in cellular viability is only observed for the experiment performed at 40°C. Although nutrient starvation has not been associated with cell death, it has been reported that cells subjected to adverse conditions, such as starvation, lose the ability to reproduce entering in a "viable but non culturable" state.[47] This state has been found to have a profound effect on bacterial cells, that associated with other stress conditions during the cultivation, might induce cellular damages leading to death.

The lower productivities observed at 27°C are also associated with lower growth and glucose uptake rates as observed in Figure 3. In fact, it is clear that, although the final levels of biomass are higher at 27°C, the rates of biomass formation are lower, which in turn explains the lower levels of acetate accumulation. A possible explanation is related to the nonoptimal enzyme activities at 27°C, reducing the whole metabolic activity in bacterial cells. Additionally, nonoptimal growth temperatures are recognized to induce physiological protective mechanisms on microorganisms.[48] One of those mechanisms triggered by low temperatures is the adjustment of the membrane lipid composition in order to ensure membrane function, such as solute transport.[48,49] Therefore, the redirection of the carbon supply to balance the membrane maintenance requirements can be a further explanation supporting the fermentation profile at 27°C.

It has also been reported that the production of recombinant proteins interferes with cellular processes in many ways.[7] Drainage of precursors and energy urges the cell to readjust metabolic fluxes inducing stress responses, and hence the cellular activity is shifted from growth to reorganization of biomass, eventually resulting in inhibition of growth. In this work, the relationship between high product and low biomass accumulation seems to be not so severe, since the final biomass formation only slightly decreased from 2.04 to 1.57 g/kg DCW when fermentations were performed at 27 and 40°C, respectively. Furthermore, as discussed above, the levels of cell injury observed at 40°C are not negligible and can definitely lead to lower biomass accumulation levels. Additionally, the increased level of acetate production during the fermentation performed at 40°C (1.58 g/kg, the maximum value achieved) can partly explain the lower levels of final biomass concentration due to the lower biomass yields observed when glucose is not totally oxidized. Moreover, the reported adverse effects of acetate in recombinant protein production[50] were not observed for this experiment.

In summary, it can be concluded that, at least for the expression system studied here, although higher temperatures provoke an increase in cellular injury, more pronounced in

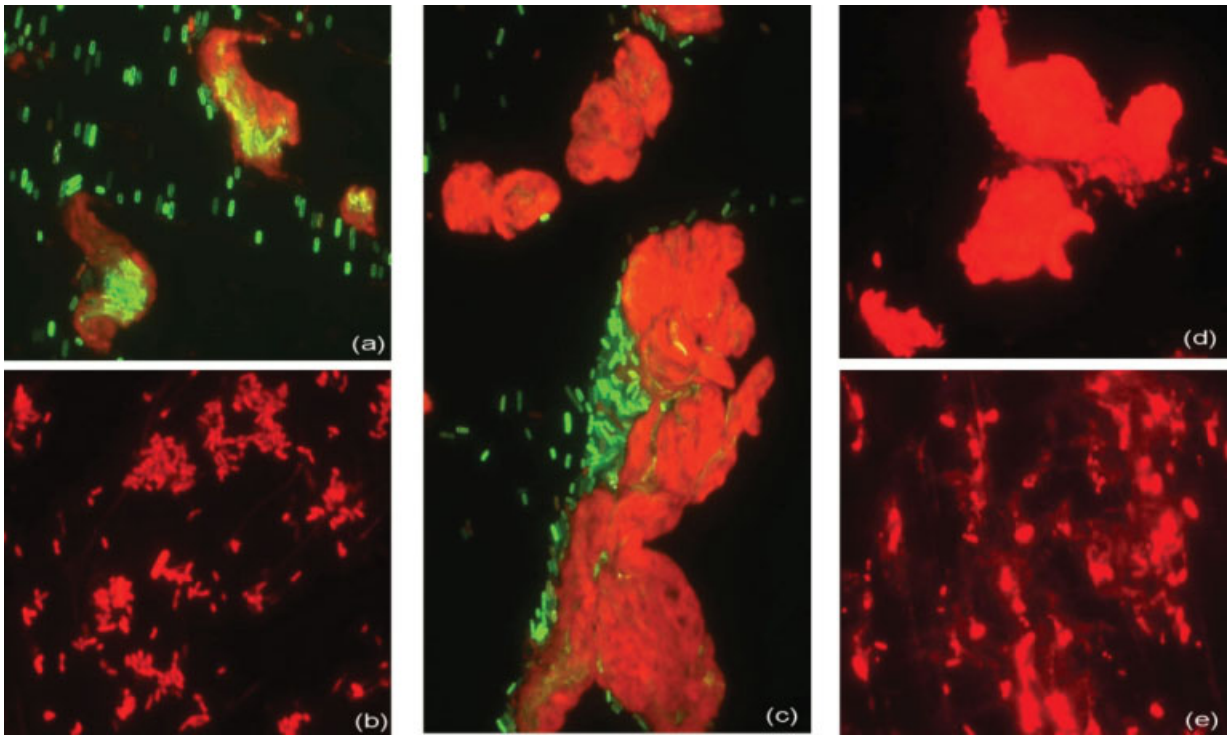

Figure 4. ***E. coli*** **EFM observations during fermentation processes.**

(a) Aggregate of nucleic acid material fused with EYFP resulting from cell lysis. (b) PI-stained cells aggregates. (c) Massive aggregation of nucleic acid material entrapping $EYFP^+$ cells. (d) Characteristic aggregates of DNA formed after lysis when inducing EYFP expression with IPTG. (e) Lysate pattern occurred immediately after IPTG addition.

$EYFP^+$ cells, recombinant protein expression is enhanced, probably due to enzymatic activities closer to optimum. This phenomenon also originates higher growth rates and higher levels of acetate accumulation. Moreover, as opposed to what has been described,[50] recombinant protein production does not interfere with growth rates and acetate accumulation seems not to inhibit the recombinant protein production.

Detection of cell lysis and aggregation by EFM

In addition to the application of image analysis tools, direct and qualitative evaluation of physiological conditions using microscopy can be very useful to investigate the occurrence of some events, like cell lysis and aggregation, as shown in Figure 4.

Cell lysis was observed in all cultures and more significantly when a stable EYFP production was achieved. As depicted, there is a relation between the existence of stress circumstances, like IPTG addition with loss of bacterial viability. The observation of cellular lysates 2–3 hr after induction (Figures 4d,e) is coherent with the decline of the injured cell ratios (Figure 3).

Other interesting phenomena were observed, like the formation of huge agglomerations of nucleic acids involving other cell components (like EYFP) or even viable cells, as illustrated in Figures 4a,c. This observation is possible with EFM since the fluorescent markers used allow a good visualization of this mixed EYFP/DNA aggregates.

Cell aggregation is not yet well understood in liquid cultivations and it is not clear if it should be regarded as a cell procedure to protect itself from chemical, biological or environmental stresses or if, on the other hand, it is a consequence of the cellular lysis that results from those stress conditions.[51] In fact, after lysis, the released DNA can be expanded, therefore promoting the formation of aggregates in the fermentation broth.

Interestingly, during the experiments performed, those events were mainly detected for fermentation D after induction and when the PI^+EYFP^+ cell ratio was around 40% of total cells. Thus, the extent of cell aggregation, besides being remarkably related with stress responses, is apparently a consequence of viability loss and not a response to stress conditions.

Evaluation of Production Patterns

Regarding the performance of recombinant protein production fermentations, EFM and image analysis tools, although not intended to be alternatives to standard methodologies such as fluorimetry or SDS-PAGE, can be regarded as further valuable tools to determine certain production parameters, like the evaluation of production patterns within a population (available as Supp. Info.).

Conclusions

In this work we report the development and application of an image analysis-based methodology for the evaluation of physiological parameters associated with cell viability and protein production during recombinant fermentation processes with *Escherichia coli*. The information obtained with such techniques, combined with standard fermentation data, allows the derivation of interesting hypothesis that can be used afterwards for experimental design and further

validation. For the case studies analyzed here, it allowed moving one step further in direct evaluation of culture physiology, discussing the effects that both the induction time and temperature have on the viability state of individual cells.

From the data presented here, it is obvious that the fermentation profiles of recombinant *E. coli* correlate well with changes in physiological conditions, as estimated by image analysis. Furthermore, IPTG induction, temperature and recombinant protein production itself exert physiological changes on the host cell.

Additionally, the cell ratios calculated in this work can be complemented with other parameters that can be extracted from image analysis. Cell aggregation and lysis occurring during fermentation processes can be observed by microscopy and generate valuable information in the evaluation of occurring stress events. These phenomena can be used as indicative of metabolic perturbations, resulting from adverse conditions.

Other methodologies that have been used to assess the physiological conditions during recombinant protein production processes, like flow cytometry, are obviously significantly faster than any microscopy method, and also provide data with much higher statistical accuracy. Nevertheless, such methods are usually less common than microscopic equipments in fermentation facilities. Also, flow cytometry does not give directly information regarding cell aggregation or lysis. Additionally, the methodology developed here allows identifying four different populations, allowing for example, to distinguish among viable cells, the fraction that is producing recombinant proteins, a feature that can only be achieved with very sophisticated flow cytometers.

A note of caution is related with the effect of the method for evaluating the viability (PI) in the results obtained. The use of other stains which evaluate the metabolic activity is considered for future work, in order to validate the results obtained with the described methodology. Furthermore, it might be still important to evaluate the fraction of "viable but nonculturable" cells for physiological studies.

Finally, it should be stated that the methodology developed here can be used for assessing both the viability and production patterns not only for the production system described but for a variety of systems, as very often the target protein can be fused with fluorescent proteins to facilitate its quantification. This methodology can also be used to study and validate novel expression systems in an expedite way.

Acknowledgments

The authors are most grateful to the Portuguese Science Foundation (FCT) by the financial support obtained under the scope of the recSysBio project (reference FCT POCI/BIO/60139/2004). Credits are also due to the remaining BioPSE group members for fruitful discussion and relevant suggestions.

Literature Cited

1. Baneyx F. Recombinant protein expression in *Escherichia coli*. *Curr Opin Biotechnol*. 1999;10:411–421.
2. Jana S, Deb JK. Strategies for efficient production of heterologous proteins in *Escherichia coli*. *Appl Microbiol Biotechnol*. 2005;67:289–298.
3. Dyson MR, Shadbolt SP, Vincent KJ, Perera RL, McCafferty J. Production of soluble mammalian proteins in *Escherichia coli*: identification of protein features that correlate with successful expression. *BMC Biotechnol*. 2004;4:32.
4. Choi JH, Keum KC, Lee SY. Production of recombinant proteins by high cell density culture of *Escherichia coli*. *Chem Eng Sci*. 2006;61:876–885.
5. Kosinski MJ, Rinas U, Bailey JE. Isopropyl-β-D-Thiogalactopyranoside influences the metabolism of *Escherichia coli*. *Appl Microbiol Biotechnol*. 1992;36:782–784.
6. Lewis G, Taylor IW, Nienow AW, Hewitt CJ. The application of multi-parameter flow cytometry to the study of recombinant *Escherichia coli* batch fermentation processes. *J Ind Microbiol Biotechnol*. 2004;31:311–322.
7. Bonomo J, Gill RT. Amino acid content of recombinant proteins influences the metabolic burden response. *Biotechnol Bioeng*. 2005;90:116–126.
8. Lin HY, Hoffmann F, Rozkov A, Enfors SO, Rinas U, Neubauer P. Change of extracellular cAMP concentration is a sensitive reporter for bacterial fitness in high-cell-density cultures of *Escherichia coli*. *Biotechnol Bioeng*. 2004;87:602–613.
9. Enfors SO, Jahic M, Rozkov A, Xu B, Hecker M, Jurgen B, Kruger E, Schweder T, Hamer G, O'Beirne D, Noisommit-Rizzi N, Reuss M, Boone L, Hewitt C, McFarlane C, Nienow A, Kovacs T, Tragardh C, Fuchs L, Revstedt J, Friberg PC, Hjertager B, Blomsten G, Skogman H, Hjort S, Hoeks F, Lin HY, Neubauer P, van der Lans R, Luyben K, Vrabel P, Manelius A. Physiological responses to mixing in large scale bioreactors. *J Biotechnol*. 2001;85:175–185.
10. Sachidanandham R, Gin KYH, Poh CL. Monitoring of active but non-culturable bacterial cells by flow cytometry. *Biotechnol Bioeng*. 2005;89:24–31.
11. Lee JH, Mitchell RJ, Gu MB. Enhancement of the multi-channel continuous monitoring system through the use of *Xenorhabdus luminescens lux* fusions. *Biosens Bioelectron*. 2004;20:475–481.
12. Garcia-Armisen T, Servais P. Enumeration of viable *E. coli* in rivers and wastewaters by fluorescent in situ hybridization. *J Microbiol Methods*. 2004;58:269–279.
13. Ericsson M, Hanstorp D, Hagberg P, Enger J, Nystrom T. Sorting out bacterial viability with optical tweezers. *J Bacteriol*. 2000;182:5551–5555.
14. Tims TB, Lim DV. Confirmation of viable E. coli O157:H7 by enrichment and PCR after rapid biosensor detection. *J Microbiol Methods*. 2003;55:141–147.
15. Bleve G, Rizzotti L, Dellaglio F, Torriani S. Development of reverse transcription (RT)-PCR and real-time RT-PCR assays for rapid detection and quantification of viable yeasts and molds contaminating yogurts and pasteurized food products. *Appl Environ Microbiol*. 2003;69:4116–4122.
16. Zhao WT, Yao SJ, Hsing IM. A microsystem compatible strategy for viable *Escherichia coli* detection. *Biosens Bioelectron*. 2006;21:1163–1170.
17. Simpkins SA, Chan AB, Hays J, Popping B, Cook N. An RNA transcription-based amplication technique (NASBA) for the detection of viable *Salmonella enterica*. *Lett Appl Microbiol*. 2000;30:75–79.
18. Williams SC, Hong Y, Danavall DCA, Howard-Jones MH, Gibson D, Frischer ME, Verity PG. Distinguishing between living and nonliving bacteria: evaluation of the vital stain propidium iodide and its combined use with molecular probes in aquatic samples. *J Microbiol Methods*. 1998;32:225–236.
19. Lopez C, Pons MN, Morgenroth E. Evaluation of microscopic techniques (epifluorescence microscopy, CLSM, TPE-LSM) as a basis for the quantitative image analysis of activated sludge. *Water Res*. 2005;39:456–468.
20. Maruyama F, Yamaguchi N, Kenzaka T, Tani K, Nasu M. Simplified sample preparation using frame spotting method for direct counting of total bacteria by fluorescence microscopy. *J Microbiol Methods*. 2004;59:427–431.
21. Shapiro HH. Microbial analysis at the single-cell level: tasks and techniques. *J Microbiol Methods*. 2000;42:3–16.
22. Porter J, Pickup RW. Nucleic acid-based fluorescent probes in microbial ecology: application of flow cytometry. *J Microbiol Methods*. 2000;42:75–79.
23. Nebe-von-Caron G, Stephens PJ, Hewitt CJ, Powell JR, Badley RA. Analysis of bacterial function by multi-colour fluorescence flow cytometry and single cell sorting. *J Microbiol Methods*. 2000;42:97–114.

24. Berney M, Weilenmann HU, Egli T. Flow-cytometric study of vital cellular functions in *Escherichia coli* during solar disinfection (SODIS). *Microbiology*. 2006;152:1719–1729.
25. Auty MAE, Gardiner GE, McBrearty SJ, O'Sullivan EO, Mulvihill DM, Collins JK, Fitzgerald GF, Stanton C, Ross RP. Direct in situ viability assessment of bacteria in probiotic dairy products using viability staining in conjunction with confocal scanning laser microscopy. *Appl Environ Microbiol*. 2001;67:420–425.
26. Breeuwer P, Abee T. Assessment of viability of microorganisms employing fluorescence techniques. *Int J Food Microbiol*. 2000; 55:193–200.
27. Nocker A, Camper AK. Selective removal of DNA from dead cells of mixed bacterial communities by use of ethidium monoazide. *Appl Environ Microbiol*. 2006;72:1997–2004.
28. Joux F, Lebaron P. Use of fluorescent probes to assess physiological functions of bacteria at single-cell level. *Microbes Infect*. 2000;2:1523–1535.
29. Tsien RY. The green fluorescent protein. *Ann Rev Biochem*. 1998;67:509–544.
30. Lehtinen J, Virta M, Lilius EM. Fluoro-luminometric real-time measurement of bacterial viability and killing. *J Microbiol Methods*. 2003;55:173–186.
31. Banning N, Toze S, Mee BJ. *Escherichia coli* survival in groundwater and effluent measured using a combination of propidium iodide and the green fluorescent protein. *J Appl Microbiol*. 2002;93:69–76.
32. Lehtinen J, Nuutila J, Lilius EM. Green fluorescent protein-propidium iodide (GFP-PI) based assay for flow cytometric measurement of bacterial viability. *Cytometry A*. 2004;60:165–172.
33. Su WW. Fluorescent proteins as tools to aid protein production. *Microb Cell Fact*. 2005;4:12.
34. Albano CR, Randers-Eichhorn L, Bentley WE, Rao G. Green fluorescent protein as a real time quantitative reporter of heterologous protein production. *Biotechnol Prog*. 1998;14:351–354.
35. Sarramegna V, Talmont F, de Roch MS, Milon A, Demange P. Green fluorescent protein as a reporter of human μ-opioid receptor overexpression and localization in the methylotrophic yeast *Pichia pastoris*. *J Biotechnol*. 2002;99:23–39.
36. Lowder M, Unge A, Maraha N, Jansson JK, Swiggett J, Oliver JD. Effect of starvation and the viable-but-nonculturable state on green fluorescent protein (GFP) fluorescence in GFP-tagged *Pseudomonas fluorescens* A506. *Appl Environ Microbiol*. 2000; 66:3160–3165.
37. Sieracki ME, Johnson PW, Sieburth JM. Detection, enumeration, and sizing of planktonic bacteria by image-analyzed epifluorescence microscopy. *Appl Environ Microbiol*. 1985;49:799–810.
38. Pons MN, Drouin JF, Louvel L, Vanhoutte B, Vivier H, Germain P. Physiological investigations by image analysis. *J Biotechnol*. 1998;65:3–14.
39. Thomas CR, Paul GC. Applications of image analysis in cell technology. *Curr Opin Biotechnol*. 1996;7:35–45.
40. Rocha I, Ferreira EC. On-line simultaneous monitoring of glucose and acetate with FIA during high cell density fermentation of recombinant *E. coli*. *Anal Chim Acta*. 2002;462:293–304.
41. Laemmli UK. Cleavage of structural proteins during assembly of head of bacteriophage-T4. *Nature*. 1970;227:680–685.
42. Yu HM, Shi Y, Sun XD, Luo H, Shen ZG. Effect of poly(beta-hydroxybutyrate) accumulation on the stability of a recombinant plasmid in *Escherichia coli*. *J Biosci Bioeng*. 2003;96:179–183.
43. Ballester S, Lopez P, Espinosa M, Alonso JC, Lacks SA. Plasmid structural instability associated with Pc194 replication functions. *J Bacteriol*. 1989;171:2271–2277.
44. Ganusov VV, Brilkov AV. Estimating the instability parameters of plasmid-bearing cells. I. Chemostat culture. *J Theor Biol*. 2002;219:193–205.
45. Yuan H, Yang X, Hua ZC. Optimization of expression of an Annexin V-Hirudin chimeric protein in *Escherichia coli*. *Microbiol Res*. 2004;159:147–156.
46. Andersson L, Yang S, Neubauer P, Enfors S-O. Impact of plasmid presence and induction on cellular responses in fed batch cultures of *Escherichia coli*. *J Biotechnol*. 1996;46:255–263.
47. Nystrom T. Not quite dead enough: on bacterial life, culturability, senescence, and death. *Arch Microbiol*. 2001;176:159–164.
48. Beales N. Adaptation of microorganisms to cold temperatures, weak acid preservatives, low pH, and osmotic stress: a review. *Compr Rev Food Sci Food Saf*. 2004;3:1–20.
49. Russell NJ, Evans RI, terSteeg PF, Hellemons J, Verheul A, Abee T. Membranes as a target for stress adaptation. *Int J Food Microbiol*. 1995;28:255–261.
50. Farmer WR, Liao JC. Reduction of aerobic acetate production by *Escherichia coli*. *Appl Environ Microbiol*. 1997;63:3205–3210.
51. Monier JM, Lindow SE. Frequency, size, and localization of bacterial aggregates on bean leaf surfaces. *Appl Environ Microbiol*. 2004;70:346–355.

Manuscript received July 28, 2008, and revision received Aug. 6, 2008.